Am J Cancer Res 2026;16(3):966-984
www.ajcr.us /ISSN:2156-6976/ajcr0168996

Original Article

CBX3 promotes epithelial-mesenchymal transition in synovial sarcoma via the SHH signaling pathway

Yachao Sun, Zhibing Dai, Junwei Du, Maierdanjian Maihemuti, Suzhi Ji, Renbing Jiang

Department of Bone and Soft Tissue Neoplasms and Melanoma, The Affiliated Cancer Hospital of Xinjiang Medical University, Urumqi 830011, Xinjiang, China

Received September 24, 2025; Accepted January 25, 2026; Epub March 25, 2026; Published March 30, 2026

Abstract: Synovial sarcoma (SS) is a malignant mesenchymal tumor of uncertain histogenesis, representing approximately 5% to 10% of all soft tissue sarcomas. It predominantly affects adolescents and young adults. The role of CBX3 (Chromobox homolog 3) in Synovial sarcoma progression, particularly in relation to epithelial mesenchymal transition (EMT), remains unclear. This study aimed to investigate the functional role of CBX3 in synovial sarcoma and to elucidate the underlying molecular mechanisms by which it regulates EMT. Human synovial sarcoma cell lines (SYO-1, HS-SY-II, YaFuSS, and Fuji) and the immortalized human keratinocyte line (HaCaT) were used for *in vitro* studies. For *in vivo* modeling, mice were inoculated with Fuji cells. CBX3 expression was significantly upregulated in human synovial sarcoma tumor specimens compared to control tissues. Clinically, patients with high CBX3 expression exhibited significantly shorter overall survival than those with low expression. In vitro, CBX3 promoted cell proliferation, induced EMT, and suppressed mitochondrial oxidative metabolism. Conversely, siRNA-mediated knockdown of CBX3 (si-CBX3) enhanced mitochondrial oxidative activity. Moreover, CBX3 overexpression inhibited ferroptosis in SS cells, whereas its knockdown (sh-CBX3) promoted both ferroptosis and mitochondrial oxidation - effects consistently observed in both in vitro assays and the mouse xenograft model. Mechanistically, CBX3 activated the Sonic Hedgehog (SHH) signaling pathway. Pharmacological inhibition of SHH signaling abrogated CBX3-mediated suppression of ferroptosis and restoration of mitochondrial oxidation. Furthermore, co-immunoprecipitation assays demonstrated that CBX3 physically interacts with SHH protein and stabilizes it by reducing its polyubiquitination. CBX3 drives EMT and tumor progression in SS by activating the SHH/Gli1 signaling axis. Mechanistically, CBX3 binds directly to and SHH and prevents its ubiquitin-mediated degradation, thereby stabilizing the protein. CBX3-SHH subsequently suppresses mitochondrial oxidative metabolism, which in turn inhibits ferroptosis and facilitates EMT - ultimately promoting SS aggressiveness.

Keywords: CBX3, Synovial sarcoma, epithelial mesenchymal transition, ferroptosis, mitochondrial oxidation

Introduction

Synovial sarcoma (SS) is a malignant mesenchymal neoplasm of uncertain histogenesis, accounting for 5% to 10% of all soft tissue tumor sarcomas and predominantly affecting adolescents and young adults [1]. Histologically, SS is defined by its biphasic differentiation pattern, featuring both mesenchymal and epithelial components. It is classified into four main subtypes: biphasic, spindle cell (monophasic), monophasic epithelial, and poorly differentiated [2]. Among these, the spindle cell variant poses a particular diagnostic challenge in pediatric patients due to its substantial histomorphological and immunophenotypic overlap with other childhood spindle cell tumors, resulting in a high risk of misdiagnosis [3].

Epithelial-mesenchymal transition (EMT) is a dynamic cellular reprogramming process through which epithelial cells lose their apicobasal polarity and cell-cell phenotype, acquiring instead a mesenchymal phenotype characterized by enhanced their migratory and invasive capabilities [4]. A hallmark of this transition is the downregulation of epithelial markers (such as E-cadherin encoded by CDH1) accompanied by the upregulation of mesenchymal markers (such as N-cadherin encoded by the CDH2 gene and vimentin encoded by the VIM gene) [5]. In lung cancer, EMT plays a pivotal role in tumor

https://doi.org/10.62347/YPDZ7241

metastasis, local invasion, and the development of resistance to multiple therapeutic modalities, including chemotherapy and immunotherapy, thereby establishing it as a central driver of tumorigenesis and progression [5]. Consequently, therapeutic strategies aimed at inhibiting or reversing the EMT program represent a promising avenue for improving clinical outcomes in cancer patients [6].

Ferroptosis, first described in 2012, is an iron-dependent, non-apoptotic form of regulated cell death driven by the iron-mediated peroxidation of polyunsaturated fatty acid (PUFA)-containing phospholipids [7]. Owing to its unique molecular mechanism, the induction of ferroptosis is considered a promising to overcome tumor therapy resistance [8]. Cellular susceptibility to ferroptosis is tightly linked to the metabolic state of the cell, particularly the homeostasis and metabolism of lipids, iron, and amino acids - especially cysteine and glutathione [9]. Notably, while tumor cells undergoing epithelial-mesenchymal transition (EMT) frequently acquire broad resistance to chemotherapy, targeted therapy, and immunotherapy, they may simultaneously become more vulnerable to ferroptosis. This paradoxical sensitivity underscores the therapeutic potential of ferroptosis induction in targeting aggressive cancers [10, 11]. Conversely, accumulating evidence suggests that ferroptosis itself may modulate EMT in various pathological contexts, including cancer and fibrotic diseases [12-14].

Sonic Hedgehog (SHH), a key secreted ligand of the Hedgehog family, plays crucial roles in regulating cell proliferation, invasion, and migration [15]. Canonical SHH signaling has been implicated in the pathogenesis of various malignancies, including lymphoma, gastric cancer, breast cancer, and Synovial sarcoma (SS) [16]. In SS, aberrant activation of the SHH signaling contributes to tumorigenesis and disease progression. Notably, in colorectal cancer (CRC), SHH pathway inhibition has been shown to suppress tumor growth, metastasis, and invasion while promoting apoptosis [17].

CBX3 recruits cohesin loader proteins to the sites of DNA double-strand breaks. Heterochromatin protein 1γ (HP1γ) is encoded by the CBX3 gene [18]. Epigenetic silencing represents the primary mechanism through which CBX3/HP1γ modulates gene expression. Accumulating evidence indicates that elevated mRNA and protein expression levels of CBX3/HP1γ are closely correlated with poor prognosis in patients with hepatocellular carcinoma (HCC) [19]. In tongue squamous cell carcinoma, CBX3 regulates the G1/S phase transition of the cell cycle by downregulating p21, thereby facilitating tumor cell proliferation [20]. Additionally, CBX3 exerts pivotal immunomodulatory functions. Specifically, genetic mutations in CBX3 can lead to interindividual variations in immune responses. In solid tumors, the deficiency of CBX3/HP1γ enhances the antitumor activity of CD8+ effector T cells [21]. To achieve optimal invasive potential, the function of tumor-derived chemokines undergoes corresponding alterations, which is attributed to the persistent presence of CBX3/HP1γ-deficient CD8+ effector T cells [22]. Bai et al. showed that CBX3 suppressed ferroptosis in colorectal carcinoma [22]. However, CBX3 regulated ferroptosis of SS cells was unclear. Here, this experiment investigated the effects of CBX3 in Synovial sarcoma and its molecular mechanisms of epithelial mesenchymal transition in Synovial sarcoma.

Materials and methods

Cell culture and animal model

HaCaT (No: GNHu64) purchased from Cell Bank of Typical Culture Preservation Committee of Chinese Academy of Sciences. YaFuSS (No: CVCL_L809) and Fuji cells (No: CVCL_JF82) purchased from Cellosaurus database. SYO-1 and HS-SY-II established in our laboratory. SYO-1 cells were transfected with negative or CBX3 plasmid (sc-419499-LAC, Santa Cruz Biotechnology, Inc.) using Lipofectamine 3000 (Invitrogen, CA). Fuji cells were transfected with si-nc or si-CBX3 (sc-35590, Santa Cruz Biotechnology, Inc.) using Lipofectamine 3000 (Invitrogen, CA).

The animal studies were authorized by the Animal Ethic Review Committees of our hospital. All animal experiments were strictly implemented in compliance with the NIH Guide for the Care and Use of Laboratory Animals. All BALB/c-nu thymus free nudemice (4-5 weeks, male, SPF) purchased from Animal Experiment Center of Xinjiang Medical University. ALL mice were randomly assigned as two groups: negative or sh-CBX3 group, the number of every

group = six. The maximum tumor size complied with ethical regulations. We confirm that the maximum tumor size complies with ethical regulations and requirements.

Fuji cells were transfected with negative or sh-CBX3 lentivirus (sc-35590-V, Santa Cruz Biotechnology, Inc.) using Lipofectamine 3000 (Invitrogen, CA). All mice were inoculated with Fuji cells (1×10^7 cells) as described in a previous study [23]. Mice was anesthetized by intraperitoneal injection of 50 mg/kg pentobarbital sodium, and then sacrificed by cervical dislocation. During treatment, the tumor length (a) and short diameter (b) of the tumor-bearing mice were measured every other day using a vernier caliper, and the tumor volume (V) was calculated using the formula $V = ab^2/2$. After the experiment, the tumor tissues were removed, photographed, and weighed.

ELISA and cell viability assay

4-HNE (H268-1-2), CAT (A007-1-1), MDA (A003-1-2), SOD (A001-3-2), GSH (A006-2-1), GSH-PX (A005-1-2) were performed as described in a previous study [24]. Cell viability was determined using CCK-8 assay (C0037, Beyotime) as described in a previous study [25]. Absorbance was measured on the Microplate Reader (Bio Tek, Winooski). EdU kit (C0075S, Beyotime) or LDH activity (C0016, Beyotime), Caspase3 (G01513), Caspase7 (H080) and caspase9 (G01811) were quantified Commercial reagent kit (Nanjing Jiancheng Bioengineering Research Institute) and Absorbance was measured at 450 nm using a fluorescent reader (Synergy H1 Microplate Reader, Bio Tek, Winooski). FeRhNOX-1 (Fe^{2+} indicator) kits were quantified Commercial reagent kit (SCT030, Goryo Chemical) at 450 nm. Upon specific and irreversible binding to Fe^{2+}, the probe emits orange/red fluorescence at approximately 575 nm under excitation with a 540 nm light source, and the fluorescence intensity exhibits a positive linear correlation with the Fe^{2+} concentration.

Mitochondrial ROS, membrane potential, or cobalt ion accumulation

(Mitochondrial Superoxide Assay Kit with MitoSO™ Red (S0061S, Beyotime), Enhanced mitochondrial membrane potential assay kit with JC-1 (C2003S, Beyotime) and Calcein AM Cell Activity Detection Kit (C2013S, Beyotime) at 450 nm using a fluorescent reader (Synergy H1 Microplate Reader, Bio Tek, Winooski).

Western blotting analysis and immunofluorescence

Western Blotting Analysis and Immunofluorescence were executed as literature [25]. CBX3 (1:1000, Abcam), SHH (1:1000, Abcam), Drp1 (1:1000, Abcam), GPX4 (ab125066, 1:1000, Abcam), β-actin (1:10000, AC028, Company ABclonal, Inc.) and Anti-Rabbit IgG (1:5000, GB23303, Servicebio) were used in this study. Protein was measured using an BeyoECL Plus kit (P0018S) and analyzed using an Image Lab 3.0 (BioRad Laboratories, Inc.). CBX3 (1:1000, Abcam), and SHH (1:1000, Abcam) was used for immunofluorescence analyses.

Immunohistochemical, and immunofluorescence analyses and electron microscopy

For immunohistochemical and immunofluorescence analyses, mouse tissue samples were fixed in 4% paraformaldehyde and stained as described in previous studies [26]. Samples were observed under a fluorescence microscope (Zeiss Axio Observer A1, Germany) and a transmission electron microscope (80 kV) (Hitachi H7650, Tokyo, Japan) as described in a previous study [25].

Statistical analysis

$P < 0.05$ was considered significant and evaluated using Student's t-test or one-way analysis of variance (ANOVA) followed by Tukey's post-test by GraphPad Prism. Data were expressed as mean ± standard deviation (SD).

Results

CBX3 expression in Synovial sarcoma and its clinical relevance

First, this study sought to identify key molecular drivers involved in the pathogenesis and progression of SS. CBX3 expression was significantly upregulated in SS tumor tissues compared with normal control tissues (**Figure 1A-C**). Clinically, patients with high CBX3 expression exhibited significantly shorter overall survival than those with CBX3 low expression (**Figure 1D**). Consistent with these find-

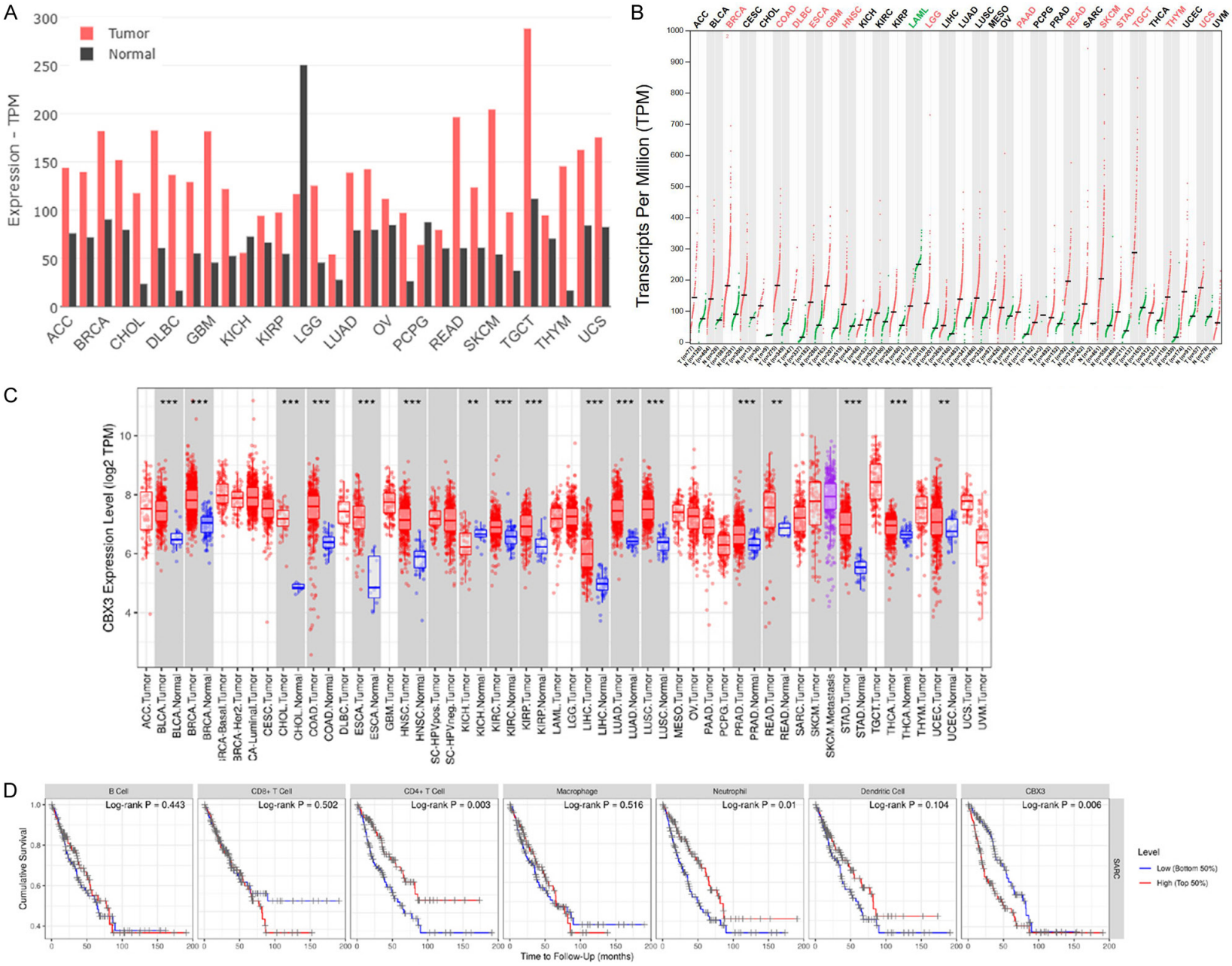
A
Tumor
Normal
Expression - TPM
ACC BRCA CHOL DLBC GBM KICH KIRP LGG LUAD OV PCPG READ SKCM TGCT THYM UCS
B
Transcripts Per Million (TPM)
C
CBX3 Expression Level (log2 TPM)
D
B Cell
Log-rank P = 0.443
CD8+ T Cell
Log-rank P = 0.502
CD4+ T Cell
Log-rank P = 0.003
Macrophage
Log-rank P = 0.516
Neutrophil
Log-rank P = 0.01
Dendritic Cell
Log-rank P = 0.104
CBX3
Log-rank P = 0.006
Cumulative Survival
Time to Follow-Up (months)
Level
Low (Bottom 50%)
High (Top 50%)

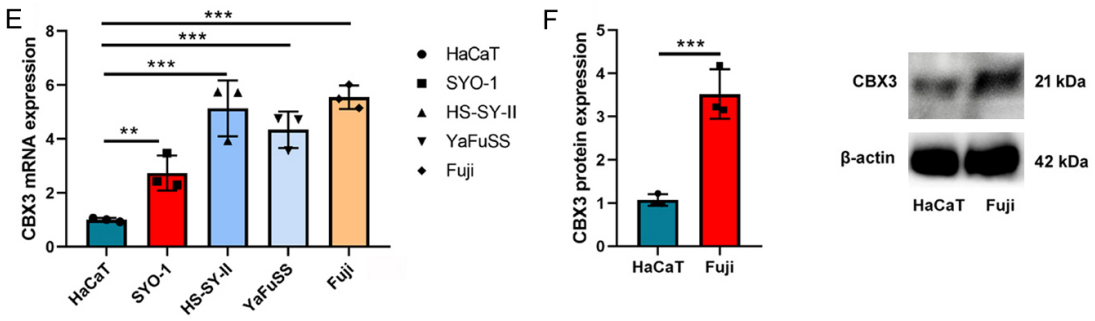

Figure 1. CBX3 expression level in patients with Synovial sarcoma. CBX3 expression was in patients with various tumor samples (A-C); Survival time (D); CBX3 mRNA and protein expressions in cells lines (E, F). **, P < 0.01; ***, P < 0.001.

ings, both mRNA and protein levels of CBX3 were markedly elevated in human SS tumor specimens and SS-derived cell lines (**Figure 1E**, **1F**).

To further characterize the cellular context of CBX3 expression, we performed single-cell RNA sequencing (scRNA-seq) to dissect the tumor microenvironment of SS. Analysis of scRNA-seq data revealed that CBX3 was predominantly enriched in the epithelial-mesenchymal compartment of SS tumors (**Figure 2A**, **2B**). In contrast, CBX3 was found to be expressed in epithelial mesenchymal of Synovial sarcoma patients (**Figure 2C**). In these datasets, CBX3 expression was minimal or absent in immune cell populations, including B cells, T cells and macrophage (**Figure 2D**, **2E**), indicating a cell type-specific expression pattern restricted to the neoplastic mesenchymal/epithelial lineage rather than stromal or immune components.

Sh-CBX3 reduced EMT and tumor growth in mouse model of Synovial sarcoma

To functionally evaluate the role of CBX3 in SS progression, we established a mouse xenograft model using SS cells stably expressing shRNA targeting CBX3 (sh-CBX3). Compared with the control group, ice bearing sh-CBX3 - expressing tumors exhibited a significant reduction in both tumor volume and weight (**Figure 3**). Furthermore, knockdown of CBX3 elevated the activities of caspase-3/7/9 in tumor tissues, downregulated mRNA expression of Cox2, TNF-α and Myc, and upregulated TP53 mRNA expression (**Figure 3**). Collectively, these findings suggest that CBX3 depletion attenuates EMT-like features and enhances pro-apoptotic signaling in SS tumors.

CBX3 promoted Synovial sarcoma cell proliferation and migration in vitro

To investigate the functional role of CBX3 in SS cells, we modulated its expression in vitro. CBX3 up-regulation significantly elevated CBX3 mRNA expression and enhanced cell proliferation (**Figure 4A**, **4B**). Conversely, siRNA-mediated knockdown of CBX3 (si-CBX3) markedly reduced CBX3 mRNA expression and suppressed cell growth in SS cells (**Figure 4C**, **4D**). Consistent with these observations, CBX3 overexpression promoted cell migration, whereas si-CBX3 treatment significantly decreased both EdU incorporation - indicative of reduced DNA synthesis - and migratory capacity (**Figure 4E-H**).

CBX3 reduced mitochondrial oxidative activity and lipid peroxidation

We next investigated whether CBX3 regulates mitochondrial function and oxidative stress. CBX3 up-regulation elevated mitochondria CoCl2 levels and JC-1 assay levels, while reducing mitochondrial ROS production and markers of mitochondrial damage (**Figure 5A-D**). Moreover, CBX3 overexpression significantly decreased the levels of lipid peroxidation end-products-4-hydroxynonenal (4-HNE) and MDA - and enhanced the activities of key antioxidant enzymes, including CAT, SOD, and GPx (**Figure 5E-I**).

Si-CBX3 enhances mitochondrial oxidation and promotes oxidative stress

In contrast, CBX3 down-regulation decreased mitochondria CoCl2 levels and JC-1 assay levels, promoted ROS production and mitochondrial damage (mitochondrial damage) in an in vitro model of Synovial sarcoma (**Figure 6A-D**). Furthermore, CBX3 down-regulation significantly increased 4-HNE, and MDA level, and reduced CAT, SOD and GSH-PX levels in an in vitro model of SS (**Figure 6E-I**).

CBX3 reduced ferroptosis in Synovial sarcoma cells

To investigate the role of CBX3 in regulating mitochondrial oxidation-induced ferroptosis in SS, we modulated CBX3 expression in SS cell lines in vitro. In an in vitro model of SS, CBX3 up-regulation significantly reduced intracellular Iron concentration, decreased levels of FeRhNOX-1 levels and Ferrous iron level, inhibited LDH activity levels, and enhanced GSH activity and GPX4 protein expression (**Figure 7A-E**, **7K**). Conversely, siRNA-mediated knockdown of CBX3 (si-CBX3) increased intracellular iron accumulation, elevated FeRhNOX-1 and ferrous iron levels, enhanced LDH release, and reduced both GSH activity and GPX4 expression (**Figure 7F-J**, **7L**). Collectively, these findings demonstrate that CBX3 suppresses ferroptosis in synovial sarcoma cells.

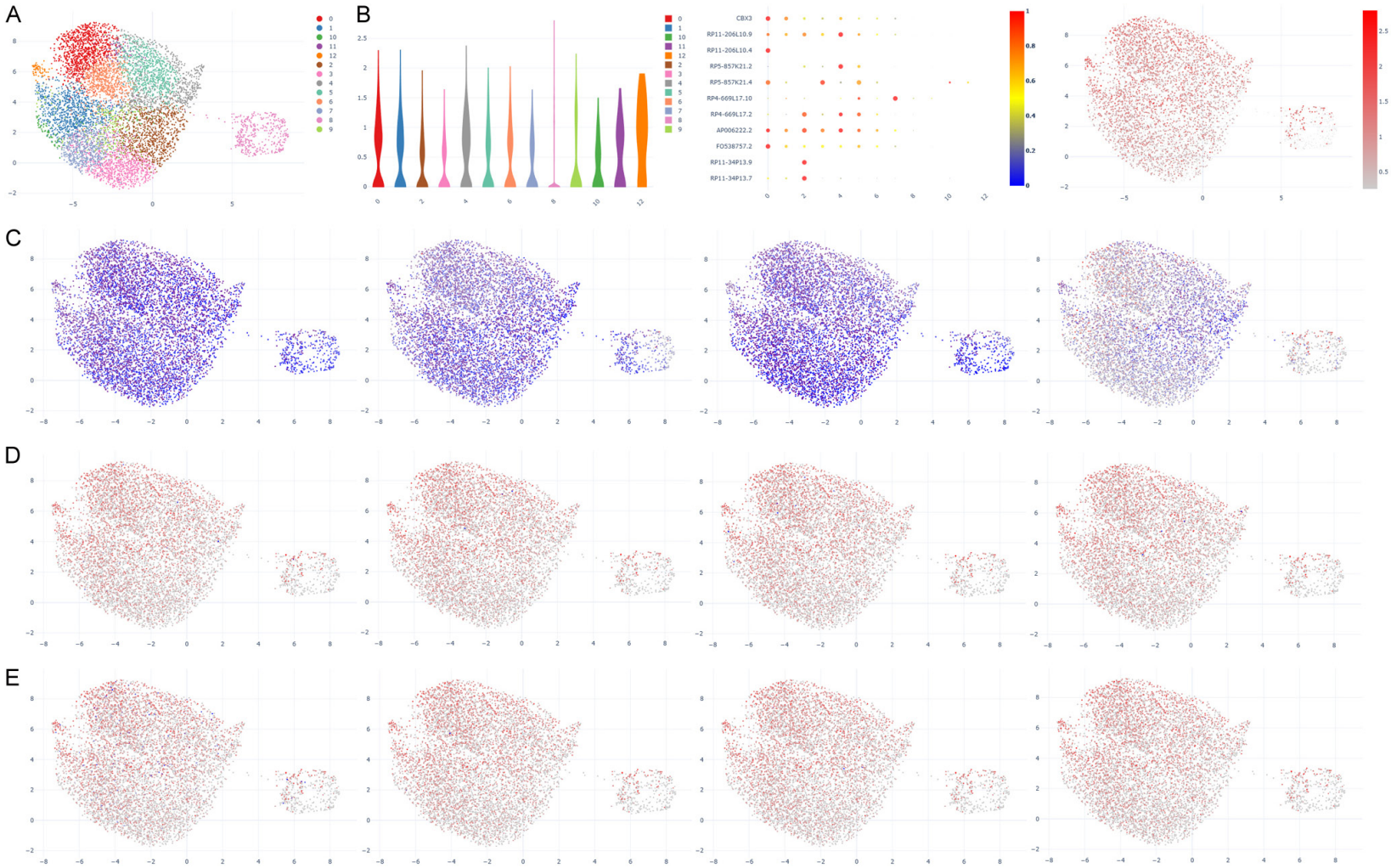

Figure 2. CBX3 expression level in epithelial mesenchymal of patients with Synovial sarcoma. Single-cell sequencing data for CBX3 expression (A, B), epithelial mesenchymal (CD24/KRT7/KRT13/MUC1, C), T/B cells (CD4, CD8A, CD83, CD86, D), macrophage (CD163/CD180/CD200/GPR171, E).

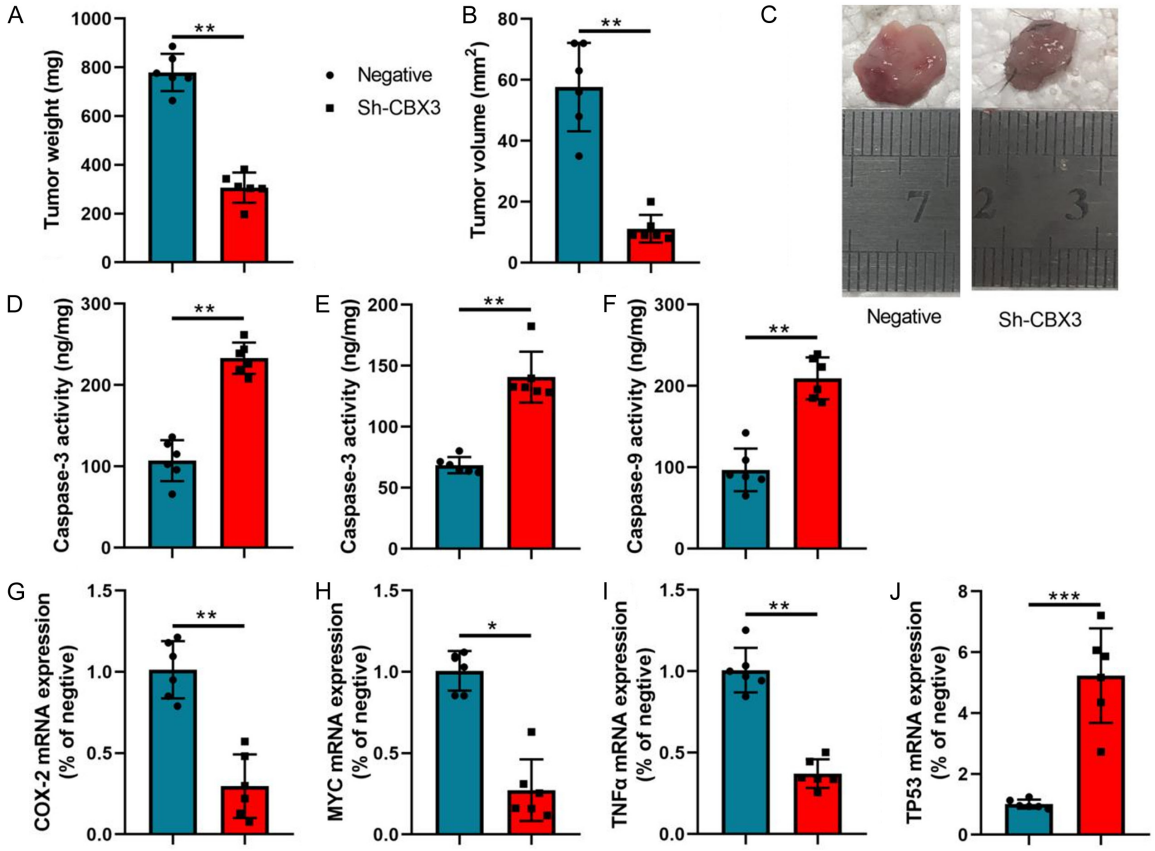

Figure 3. Sh-CBX3 reduced epithelial mesenchymal transition in mouse model of Synovial sarcoma. Tumor weight (A), volume (B), cancer tissue (C), caspase-3/7/9 activity levels (D-F), Cox2/TNF-α/MYC/TP53 mRNA expression (G-J) in mouse model. $^{**}P < 0.01$, $^{***}P < 0.001$.

Sh-CBX3 promoted ferroptosis and oxidative stress in mouse model of Synovial sarcoma

We next extended our findings to an in vivo setting. In mice bearing SS xenografts, CBX3 down-regulation (sh-CBX3) significantly promoted FeRhNOX-1 levels and Ferrous iron level, increased LDH activity levels, 4-HNE and MDA level, reduced CAT, SOD, GSH-PX and GSH levels, and suppressed GPX4 protein expressions in an in vitro model of SS (**Figure 8**). These results demonstrate that CBX3 silencing CBX3 in vivo enhances ferroptosis and fosters a pro-oxidative tumor microenvironment.

CBX3 drives EMT in synovial sarcoma

Given the established association between ferroptosis resistance and tumor progression, we sought to determine whether CBX3 regulates EMT in SS. In mouse model of Synovial sarcoma, sh-CBX3 promoted E-cadherin and ZO-1 mRNA expressions, and decreased Fibronectin, N-cadherin, Vimentin and α-SMA mRNA expressions levels in tissue samples (**Figure 9A**). Conversely, CBX3 up-regulation suppressed E-cadherin and ZO-1 mRNA expressions, and induced Fibronectin, N-cadherin, Vimentin and α-SMA mRNA expressions levels in an in vitro model of Synovial sarcoma (**Figure 9B**). Meanwhile, si-CBX3 reduced this trend in an in vitro model of Synovial sarcoma (**Figure 9C**). Together, these results demonstrate that CBX3 promotes EMT in SS.

CBX3 induced SHH/Drp1 signaling pathway in Synovial sarcoma

To investigate the molecular mechanism by which CBX3 promotes EMT, we performed gene chip screening (**Figure 10A**) and identified Sonic Hedgehog (SHH) signaling as a top candidate pathway. Sh-CBX3 reduced CBX3/SHH/Drp1 protein expressions in mouse model of Synovial sarcoma (**Figure 10B**). Immunohistochemistry and in vivo imaging showed that

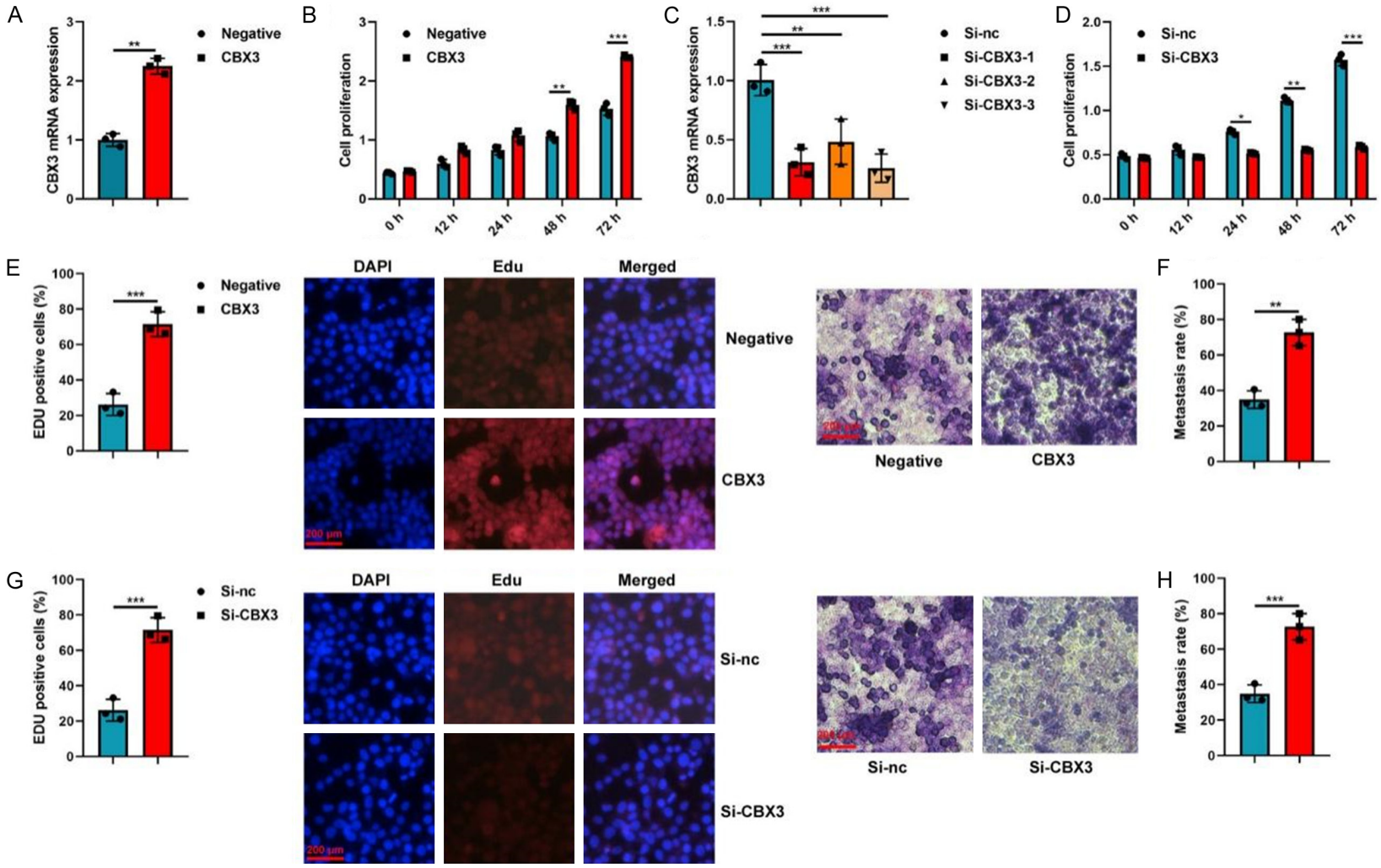

Figure 4. CBX3 promoted cell growth in vitro model of Synovial sarcoma. CBX3 expression (A), cell growth (CCK-8, B) in vitro model by CBX3 up-regulation; CBX3 expression (C), cell growth (CCK-8, D) in vitro model by si-CBX3 down-regulation; Edu positivity (E) and Migration (F) in vitro model by CBX3 up-regulation; Edu positivity (G) and Migration (H) in vitro model by CBX3 down-regulation. $^{**}P < 0.01$, $^{***}P < 0.001$.

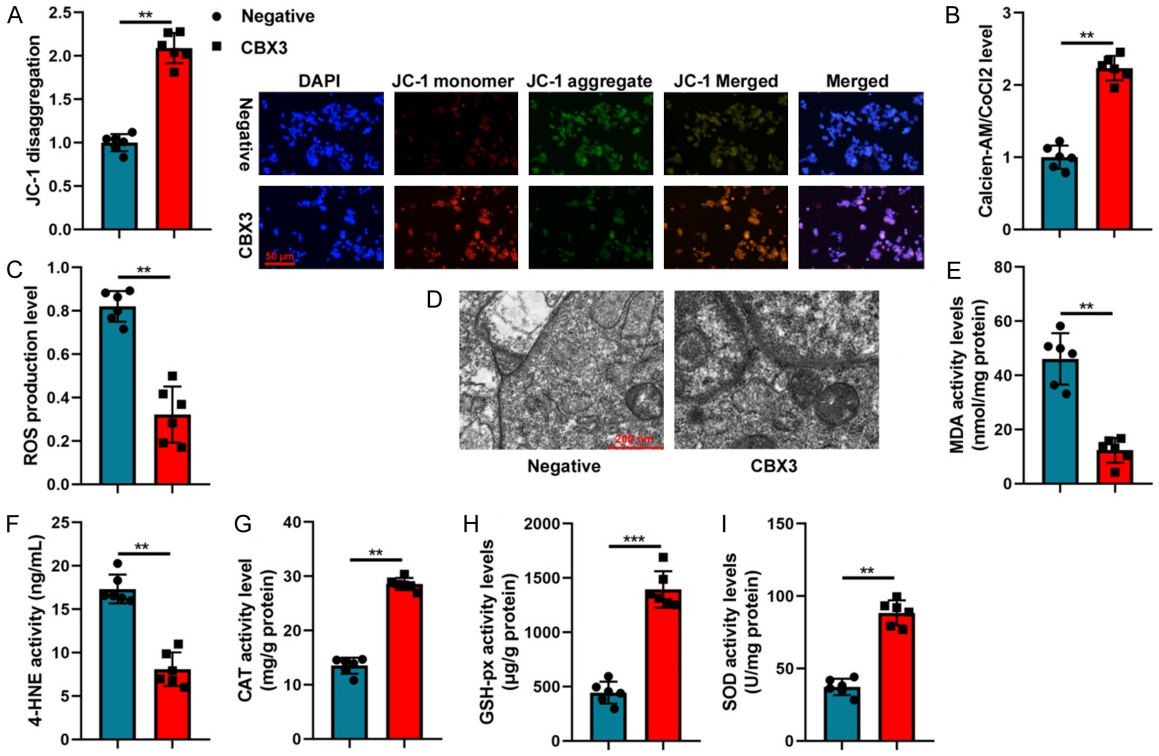

Figure 5. CBX3 reduced mitochondrial oxidation in vitro model of Synovial sarcoma. JC-1 assay (A), Mitochondria CoCl2 levels (B), ROS production level (C), Mitochondrial damage (electron microscope, D), MDA/4-HNE/CAT/GSH-PX/SOD (E-I). $^{**}P < 0.01$, $^{***}P < 0.001$.

sh-CBX3 reduced SHH expressions in mouse model of Synovial sarcoma (**Figure 10C**, **10D**). In vitro, overexpression of CBX3 (CBX3-OE) increased the protein levels of CBX3, SHH, and Drp1, whereas siRNA-mediated knockdown (si-CBX3) suppressed their expression (**Figure 10E**, **10F**). Collectively, these findings demonstrate that CBX3 positively regulates the SHH/Drp1 signaling axis in SS.

The inhibition of SHH signaling pathway attenuates CBX3-mediated suppression of ferroptosis and mitochondrial oxidation

We next investigated whether SHH signaling mediates the effects of CBX3 on ferroptosis and mitochondrial function. In an in vitro model of SS, SHH inhibitor (DS-1-38, 1 μM) significantly attenuated CBX3-induced upregulation of SHH, Drp1, and GPX4 protein levels and reversed CBX3-mediated suppression of ferroptosis (**Figure 11**). Concurrently, DS-1-38 diminished the ability of CBX3 to inhibit mitochondrial oxidative stress (**Figure 12**). These findings suggest that SHH signaling is essential for CBX3 to suppress ferroptosis and maintain a reduced mitochondrial oxidative state in SS cells.

CBX3 binds to SHH and inhibits its ubiquitination

To further elucidate the mechanism by which CBX3 activates Sonic Hedgehog (SHH) signaling, we investigated the physical interaction between CBX3 and SHH in synovial sarcoma (SS) cells. Overexpression of CBX3 (CBX3-OE) increased the protein levels of both CBX3 and SHH (**Figure 13A**).

IP analysis demonstrated that CBX3 WT protein interacts with the CBX3 WT protein, while the CBX3 WT protein does not interact with the SHH Mut protein, and the SHH Mut protein does not link with the CBX3 WT protein (**Figure 13B**). Supporting this, 3D structural modeling predicted a direct physical interface between the CBX3 and SHH proteins (**Figure 13C**). Importantly, CBX3-OE decreased the ubiquitination level of SHH protein, whereas CBX3 knockdown enhanced SHH ubiquitination (**Figure 13D**). Then, CBX3 down-regulation pro-

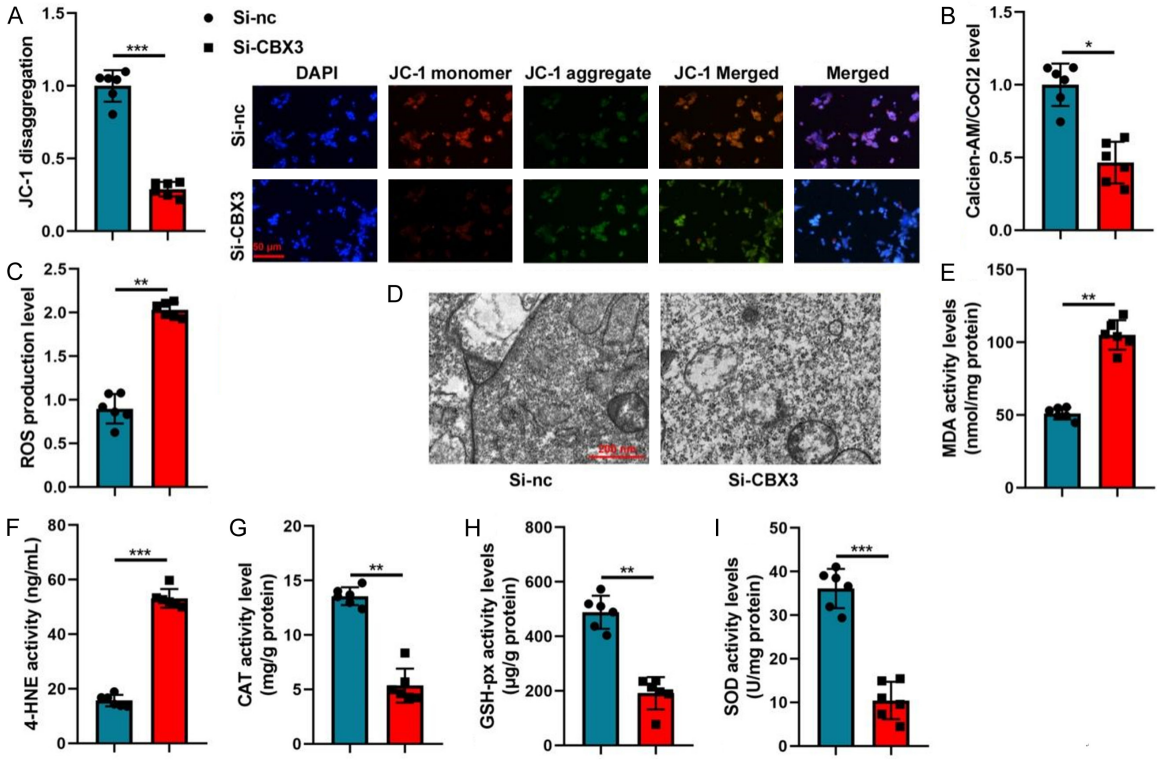

Figure 6. Si-CBX3 promoted mitochondrial oxidation in vitro model of Synovial sarcoma. JC-1 assay (A), Mitochondria CoCl2 levels (B), ROS production level (C), Mitochondrial damage (electron microscope, D), MDA/4-HNE/CAT/GSH-PX/SOD (E-I). $^{**}P < 0.01$, $^{***}P < 0.001$.

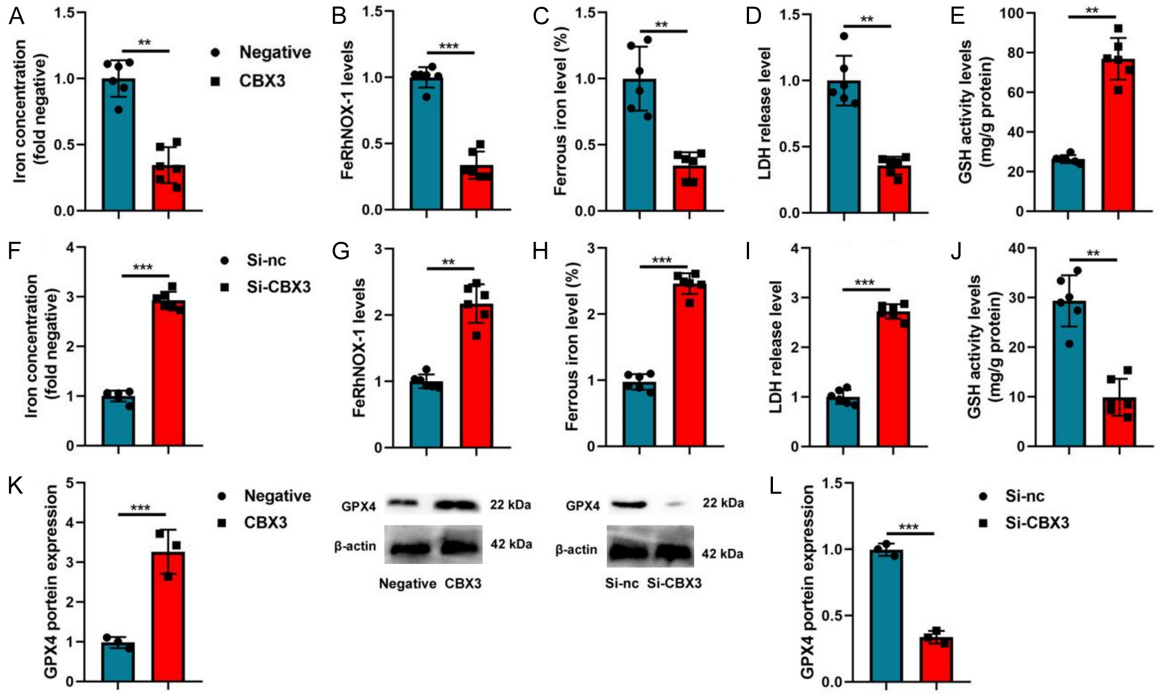

Figure 7. CBX3 reduced ferroptosis in vitro model of Synovial sarcoma. Iron concentration level (A), FeRhNOX-1 (B), Ferrous concentration level (C), LDH activity levels (D), GSH activity level (E) in vitro model by MFAP4 up-regulation; Iron concentration level (F), FeRhNOX-1 (G), Ferrous concentration level (H), LDH activity levels (I), GSH activity level (J) in vitro model by MFAP4 up-regulation; GPX4 protein expression (K, L). $^{**}P < 0.01$, $^{***}P < 0.001$.

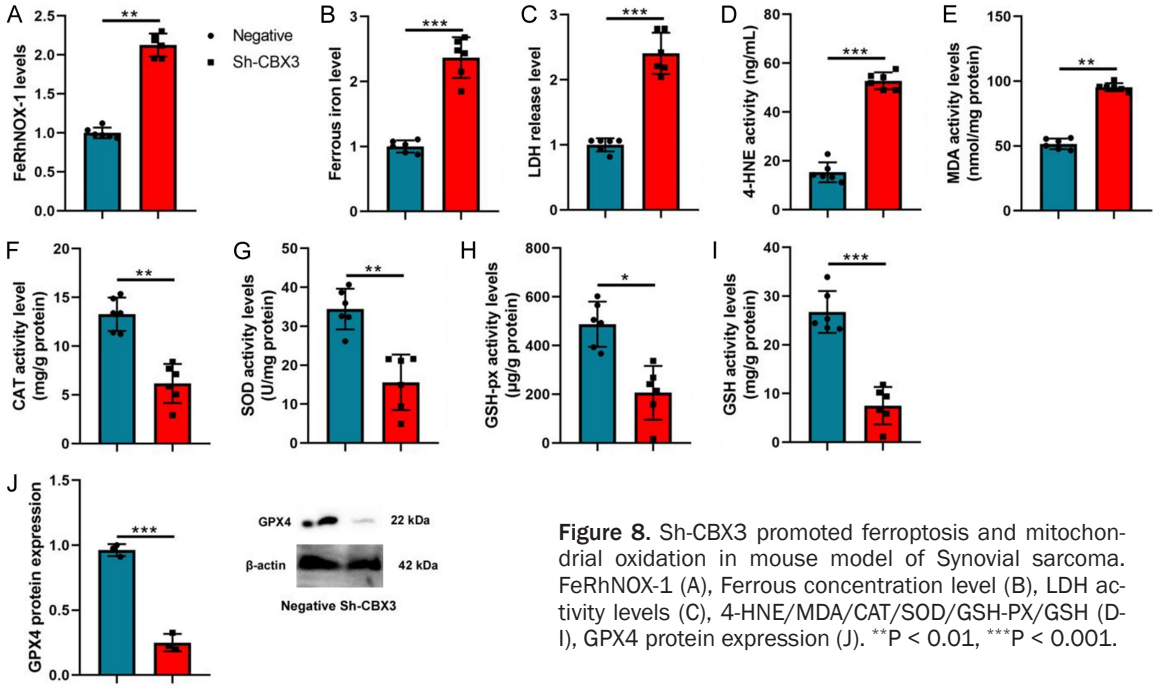

Figure 8. Sh-CBX3 promoted ferroptosis and mitochondrial oxidation in mouse model of Synovial sarcoma. FeRhNOX-1 (A), Ferrous concentration level (B), LDH activity levels (C), 4-HNE/MDA/CAT/SOD/GSH-PX/GSH (D-I), GPX4 protein expression (J). $^{**}P < 0.01$, $^{***}P < 0.001$.

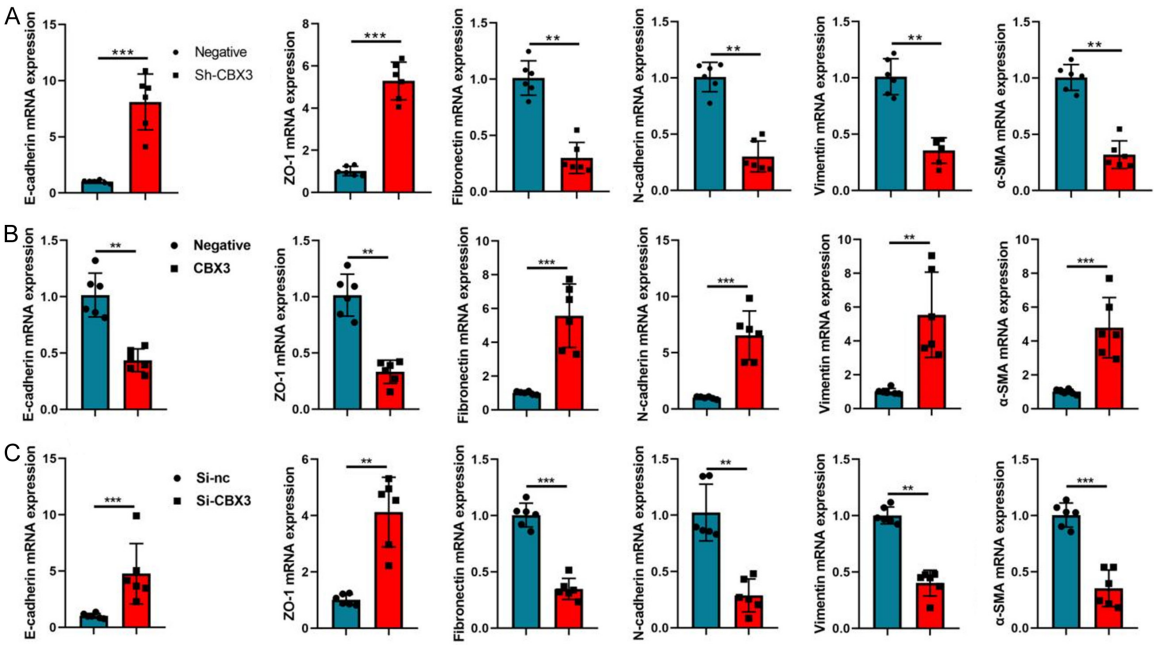

Figure 9. CBX3 promoted epithelial mesenchymal transition in model of Synovial sarcoma. E-cadherin, ZO-1, N-cadherin, Fibronectin, Vimentin, α-SMA in mouse model by sh-CBX3 (A); E-cadherin, ZO-1, N-cadherin, Fibronectin, Vimentin, α-SMA in vitro model by CBX3 (B); E-cadherin, ZO-1, N-cadherin, Fibronectin, Vimentin, α-SMA in vitro model by si-CBX3 (C). $^{**}P < 0.01$, $^{***}P < 0.001$.

moted ubiquitination of SHH protein of microglial in model of Synovial sarcoma (**Figure 13E**). Collectively, these data demonstrate that CBX3 directly binds to SHH and potentiating its signaling activity in SS.

Discussion

SS is a malignant mesenchymal tumor of uncertain tissue origin, accounting for 5%-10% of all soft tissue sarcomas [27]. It typically presents

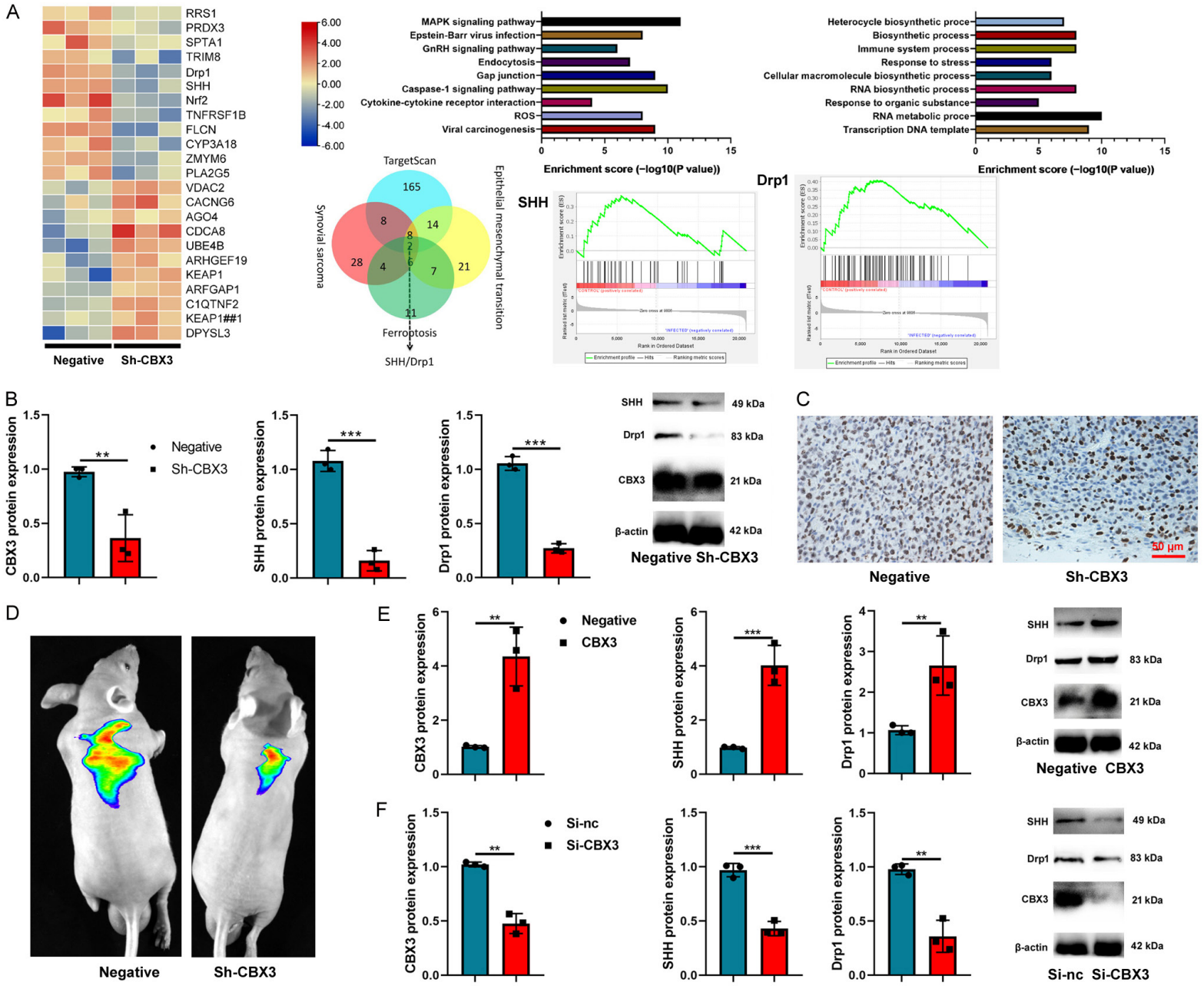
A
RRS1
PRDX3
SPTA1
TRIM8
Drp1
SHH
Nrf2
TNFRSF1B
FLCN
CYP3A18
ZMYM6
PLA2G5
VDAC2
CACNG6
AGO4
CDCA8
UBE4B
ARHGEF19
KEAP1
ARFGAP1
C1QTNF2
KEAP1##1
DPYSL3
Negative
Sh-CBX3
6.00
4.00
2.00
0.00
-2.00
-4.00
-6.00
MAPK signaling pathway
Epstein-Barr virus infection
GnRH signaling pathway
Endocytosis
Gap junction
Caspase-1 signaling pathway
Cytokine-cytokine receptor interaction
ROS
Viral carcinogenesis
Enrichment score (−log10(P value))
Heterocycle biosynthetic proce
Biosynthetic process
Immune system process
Response to stress
Cellular macromolecule biosynthetic process
RNA biosynthetic process
Response to organic substance
RNA metabolic proce
Transcription DNA template
Enrichment score (−log10(P value))
TargetScan
Synovial sarcoma
Epithelial mesenchymal transition
165
8
14
28
4
7
21
11
Ferroptosis
SHH/Drp1
SHH
Drp1
B
CBX3 protein expression
SHH protein expression
Drp1 protein expression
Negative
Sh-CBX3
SHH
Drp1
CBX3
β-actin
49 kDa
83 kDa
21 kDa
42 kDa
Negative Sh-CBX3
C
50 μm
Negative
Sh-CBX3
D
Negative
Sh-CBX3
E
CBX3 protein expression
SHH protein expression
Drp1 protein expression
Negative
CBX3
SHH
Drp1
CBX3
β-actin
83 kDa
21 kDa
42 kDa
Negative CBX3
F
CBX3 protein expression
SHH protein expression
Drp1 protein expression
Si-nc
Si-CBX3
SHH
Drp1
CBX3
β-actin
49 kDa
83 kDa
21 kDa
42 kDa
Si-nc Si-CBX3

Figure 10. CBX3 induced SHH signaling pathway in vitro model of Synovial sarcoma. Heat map (A), CBX3/SHH/Drp1 protein expression (B), SHH expression (Immunohistochemistry, C), SHH expression (in vivo imaging, D) in mouse model; CBX3/SHH/Drp1 protein expression in vitro model by CBX3 up-regulation (E) or MFAP4 down-regulation (F). $^{**}P < 0.01$, $^{***}P < 0.001$.

as a painless, slow-growing mass, most frequently located near large joints of the extremities [28]. Histologically, SS is classified into three main subtypes: monophasic, biphasic, and poorly differentiated subtypes [29]. Notably, the biphasic differentiation of SS may be related to EMT [30]. Despite advances in multimodal therapy, the prognosis prognosis of SS remains poor, with a 5-year survival rate of approximately 60% [31]. Although SS can occur across all age groups, it predominantly affects adolescents and young adults aged 15-40 years, with a peak incidence between 30 and 40 years; cases under the age of 10 are rare [32]. In this study, CBX3 expression level in patients with Synovial sarcoma was up-regulated. CBX3 expression level in epithelial mesenchymal of patients with Synovial sarcoma. Muhammad Aamir Wahab showed that CBX3 could be useful for developing novel targeted therapies for lung cancer [19]. Underscoring its broader oncogenic relevance beyond SS. Therefore, we aimed to investigate the specific role and mechanism of CBX3 in SS progression. This study did not collect clinical samples as an important part of the trial. This is also the deficiency of this study. We will continue to collect clinical samples as supporting materials for the trial in the follow-up study.

EMT is a fundamental biological process closely linked to tumor recurrence and metastasis, and poor clinical outcomes across multiple cancer types [33]. During EMT, epithelial cells lose their polarity apical-basal polarity and cell-cell adhesion properties, acquiring migratory and invasive characteristics typical of mesenchymal cells [34]. This phenotypic switch is driven by coordinated molecular changes, including downregulation of epithelial markers (e.g., E-cadherin), upregulation of mesenchymal markers (e.g., N-cadherin, vimentin), and remodeling of adhesion complexes-collectively enhancing the capacity of tumor cells to disseminate and invade distant tissues [35]. This process is closely linked to the metastasis and invasion of synovial sarcoma [36]. We found that CBX3 promoted cell growth and EMT in model of Synovial sarcoma. Chen et al. showed that CBX3 played a crucial role in enhancing EMT of cell renal carcinoma [37], further underscoring its oncogenic function in facilitating EMT across diverse malignancies. Together, these findings establish CBX3 as a potent inducer of EMT in SS.

Ferroptosis is an iron-dependent, non-apoptotic form of regulated cell death driven by the accumulation of lipid peroxidation [38, 39]. It can be induced by various physiological conditions and pathological stresses in humans and animals [40]. Early studies established that ferroptosis is mechanistically distinct from apoptosis, necrosis, and autophagy [41]. A hallmark of many cancers is the dysregulation of iron metabolism: tumor cells often upregulate iron uptake and retention to fuel rapid proliferation, which concurrently renders them susceptible to ferroptosis [42]. As a result, inducing ferroptosis has emerged as a promising strategy to eliminate therapy-resistant cancer cells, with multiple oncogenic pathways and tumor suppressors implicated in its regulation [10, 43]. Nevertheless, despite its therapeutic potential, ferroptosis research remains in its early stages in several key areas [44]. In this study, CBX3 reduced mitochondrial oxidation and ferroptosis in model of Synovial sarcoma. Bai et al. reported that CBX3 suppressing ferroptosis in colorectal carcinoma [22]. Collectively, these results indicate that CBX3 protects synovial sarcoma cells from mitochondrial oxidation - induced ferroptosis. This study found that CBX3 affects the EMT progression of Synovial Sarcoma disease by regulating ferroptosis. However, more experiments are needed in the future to confirm this and study its possible mechanisms.

Activation of Shh signaling induces the expression of its downstream effector, glioma-associated oncogene homolog 1 (Gli1) [45]. Purmorphamine (PM), a selective small-molecule agonist of the Shh pathway, has been shown to suppress forkhead box Q1 (FOXQ1)-mediated apoptosis. The Shh/Gli1 axis plays a pivotal role in numerous developmental and homeostatic processes, including the regula-

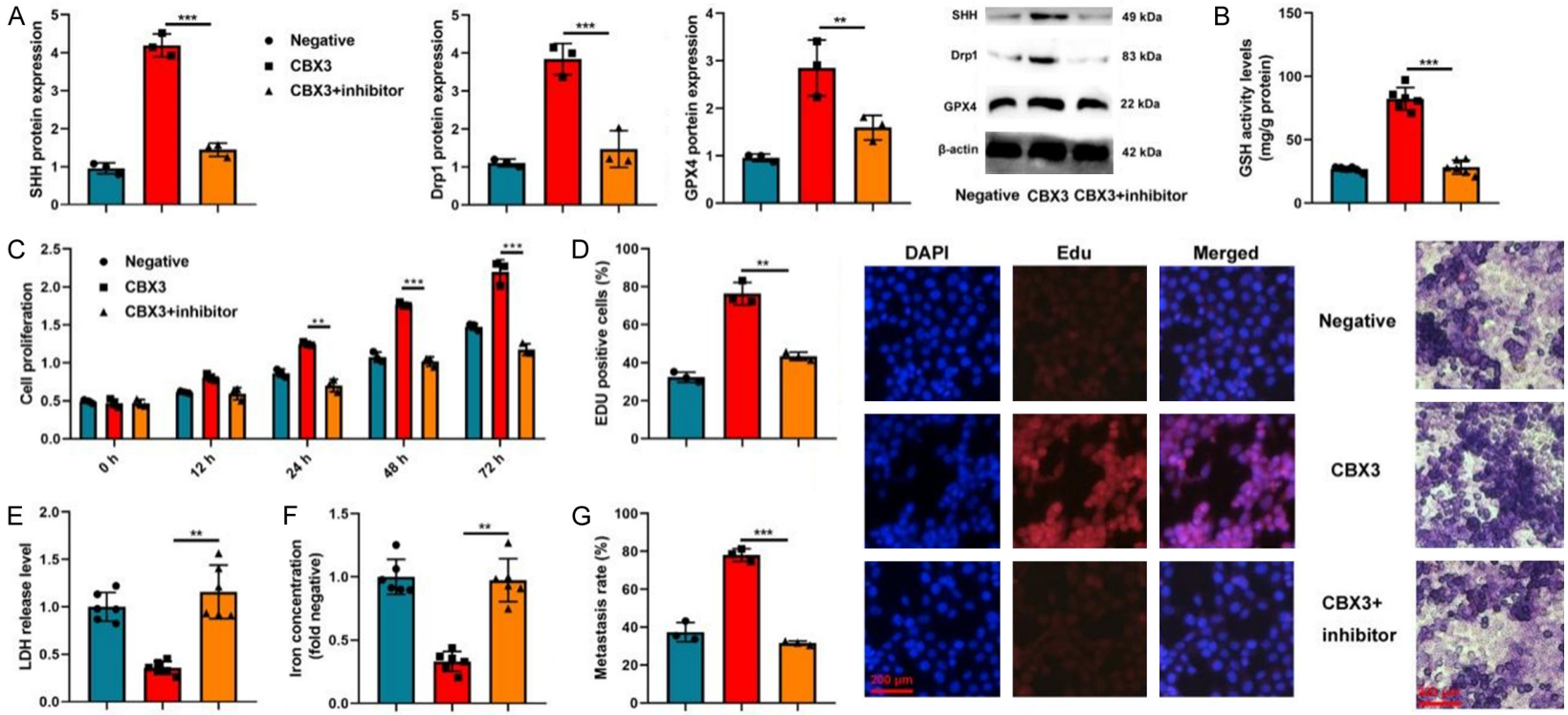

Figure 11. The inhibition of SHH signaling pathway reduced the effects of CBX3 on ferroptosis in vitro model of Synovial sarcoma. SHH/Drp1/GPX4 protein expression (A), GSH activity (B), cell growth (C), Edu positivity (D), LDH activity (E), Iron concentration level (F) and Migration (G). $^{**}P < 0.01$, $^{***}P < 0.001$.

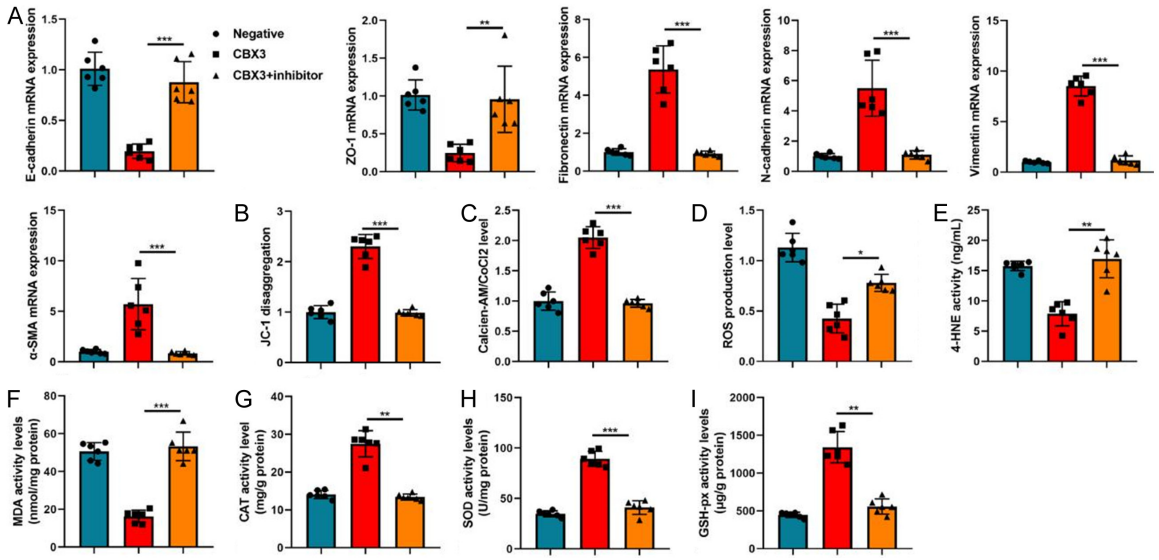

Figure 12. The inhibition of SHH signaling pathway reduced the effects of CBX3 on mitochondrial oxidation in vitro model of Synovial sarcoma. E-cadherin/ZO-1/N-cadherin/Fibronectin/Vimentin/α-SMA (A), JC-1 assay (B), Mitochondria CoCl2 levels (C), ROS production level (D), 4-HNE/MDA/CAT/SOD/GSH-PX (E-I). $^{**}P < 0.01$, $^{***}P < 0.001$.

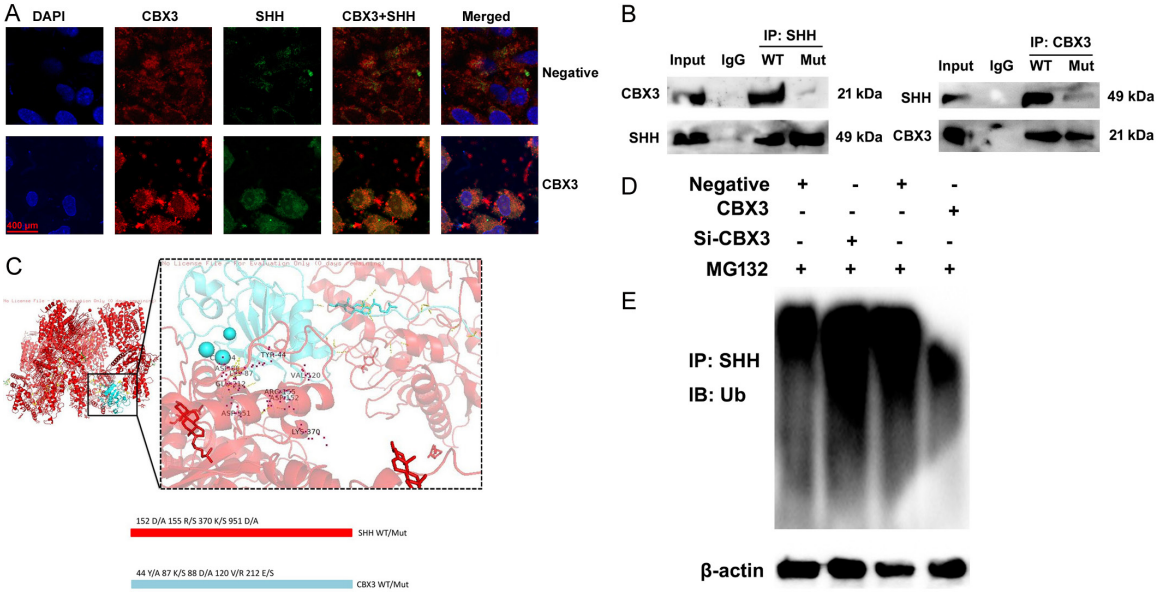

Figure 13. CBX3 protein interlinked SHH protein to reduce SHH ubiquitination in vitro model of Synovial sarcoma. CBX3/SHH expression (immunofluorescence, A), IP assay for CBX3 protein interlinking with SHH protein (B), Hdock was used to dock CBX3/SHH protein (C), CBX3/SHH WT/Mut (D), SHH ubiquitination (E).

tion of cell growth, proliferation, differentiation, survival, and tissue repair [15]. Shh participates in the regulation of embryonic development, cell proliferation, differentiation, and survival. The binding of Shh ligand to its cognate receptor triggers aberrant activation of the Shh pathway, which contributes to the metastasis and migration of multiple malignant tumors [46]. As the primary transcriptional effector of Shh signaling, Gli1 directly upregulates the expression of oncogenes involved in cell cycle progression, angiogenesis, and epithelial-mesenchymal transition [47]. Activation of the Shh pathway can induce the activation of Gli family transcription factors (primarily Gli1), cell cycle-related regulators, and angiogenesis-associat-

ed factors, thereby facilitating cell proliferation and growth. Notably, accumulating evidence indicates that the Shh/Gli1 pathway is hyperactivated during hepatocellular carcinoma progression [48], and pharmacological or genetic inhibition of Shh or Gli1 suppresses liver cancer cell proliferation, migration, and invasion while promoting apoptosis [16, 49]. Our experiment showed that CBX3 induced SHH/Grp1 signaling pathway to reduce SHH ubiquitination in vitro model of Synovial sarcoma. Furthermore, inhibition of the SHH signaling pathway abrogated the regulatory effects of CBX3 on ferroptosis and mitochondrial oxidation in this in vitro synovial sarcoma model. This study found that CBX3 induced SHH/GRP1 signaling pathway, but it is not clear whether CBX3 has other targets. This is also what we need to study in the next experiment.

In summary, our findings demonstrate that CBX3 drives SS progression by stabilizing the SHH protein through inhibition of its ubiquitin-mediated degradation. This stabilization activates the SHH/Gli1 signaling pathway, which subsequently suppresses mitochondrial oxidative metabolism and inhibits ferroptosis. The resulting attenuation of ferroptosis promotes EMT and fuels tumor growth. Collectively, these results position the CBX3-SHH axis as a promising therapeutic target in synovial sarcoma. Targeting CBX3 may therefore represent a novel and effective strategy not only for SS but potentially for other malignancies dependent on this oncogenic pathway.

Acknowledgements

This study was supported by Natural Science Foundation of Xinjiang Uygur Autonomous Region (No. 2024D01C336).

Disclosure of conflict of interest

None.

Address correspondence to: Renbing Jiang, Department of Bone and Soft Tissue Neoplasms and Melanoma, The Affiliated Cancer Hospital of Xinjiang Medical University, No. 789, East Suzhou Street, Xinshi District, Urumqi 830011, Xinjiang, China. Tel: +86-0991-7819123; E-mail: renbingjiang@outlook.com

References

[1] Fernandes S, Rastogi S, Bhatia KP, Shamim SA, Barwad A, Pandey R, Gammanagatti S and Dhamija E. Efficacy and tolerability of a low-dose continuous regimen of regorafenib in refractory synovial sarcomas: a single-arm, Phase II trial from India. JCO Glob Oncol 2025; 11: e2400558.

[2] Barnett KK, Johnson AR, Das A, Lee CJ, Wang C, Wang X, Cho ES, Kluetz PG and Fashoyin-Aje LA. FDA approval summary: afamitresgene autoleucel for adults with HLA-restricted, MAGE-A4-positive unresectable or metastatic synovial sarcoma after prior chemotherapy. Clin Cancer Res 2025; 31: 3112-3117.

[3] Acar M and Niehaus AG, Acevedo JBH and Wuertzer SD. Synovial sarcoma mimicking infrapatellar bursitis: a diagnostic challenge. Radiol Case Rep 2025; 20: 3994-3997.

[4] Manfioletti G and Fedele M. Epithelial-Mesenchymal Transition (EMT). Int J Mol Sci 2023; 24: 11386.

[5] Mittal V. Epithelial mesenchymal transition in tumor metastasis. Annu Rev Pathol 2018; 13: 395-412.

[6] Lee HW, Jose CC and Cuddapah S. Epithelial-mesenchymal transition: insights into nickel-induced lung diseases. Semin Cancer Biol 2021; 76: 99-109.

[7] Ling H, Xiao H, Luo T, Lin H and Deng J. Role of ferroptosis in regulating the epithelial-mesenchymal transition in pulmonary fibrosis. Biomedicines 2023; 11: 163.

[8] Mu W, Zhou Z, Shao L, Wang Q, Feng W, Tang Y, He Y and Wang Y. Advances in the relationship between ferroptosis and epithelial-mesenchymal transition in cancer. Front Oncol 2023; 13: 1257985.

[9] Li F, Guo L, Zhou M, Han L, Wu S, Wu L and Yang J. Cryptochrome 2 suppresses epithelial-mesenchymal transition by promoting trophoblastic ferroptosis in unexplained recurrent spontaneous abortion. Am J Pathol 2024; 194: 1197-1217.

[10] Lee J, You JH, Kim MS and Roh JL. Epigenetic reprogramming of epithelial-mesenchymal transition promotes ferroptosis of head and neck cancer. Redox Biol 2020; 37: 101697.

[11] Pu Z, Gui Y, Wang W, Shui Y, Xie H and Zhao M. Ophiopogonin D from Ophiopogon japonicas-induced USP25 activity to reduce ferroptosis of macrophage in acute lung injury by the inhibition of bound Rac1 and Nox1 complex. Am J Chin Med 2025; 53: 501-522.

[12] Liu Z, Nan P, Gong Y, Tian L, Zheng Y and Wu Z. Endoplasmic reticulum stress-triggered ferroptosis via the XBP1-Hrd1-Nrf2 pathway induces EMT progression in diabetic nephropathy. Biomed Pharmacother 2023; 164: 114897.

[13] Zhang H, Chen N, Ding C, Zhang H, Liu D and Liu S. Ferroptosis and EMT resistance in cancer: a comprehensive review of the interplay. Front Oncol 2024; 14: 1344290.

[14] Ren Y, Mao X, Xu H, Dang Q, Weng S, Zhang Y, Chen S, Liu S, Ba Y, Zhou Z, Han X, Liu Z and Zhang G. Ferroptosis and EMT: key targets for combating cancer progression and therapy resistance. Cell Mol Life Sci 2023; 80: 263.
[15] Islam SS, Mokhtari RB, Noman AS, Uddin M, Rahman MZ, Azadi MA, Zlotta A, van der Kwast T, Yeger H and Farhat WA. Sonic hedgehog (Shh) signaling promotes tumorigenicity and stemness via activation of epithelial-to-mesenchymal transition (EMT) in bladder cancer. Mol Carcinog 2016; 55: 537-551.
[16] Ghorbaninejad M, Meyfour A, Maleknia S, Shahrokh S, Abdollahpour-Alitappeh M and Asadzadeh-Aghdaei H. Inhibition of epithelial SHH signaling exerts a dual protective effect against inflammation and epithelial-mesenchymal transition in inflammatory bowel disease. Toxicol In Vitro 2022; 82: 105382.
[17] Zhang F, Ren CC, Liu L, Chen YN, Yang L, Zhang XA, Wang XM and Yu FJ. SHH gene silencing suppresses epithelial-mesenchymal transition, proliferation, invasion, and migration of cervical cancer cells by repressing the hedgehog signaling pathway. J Cell Biochem 2018; 119: 3829-3842.
[18] Wang S, Huang T, Wu Q, Yuan H, Wu X, Yuan F, Duan T, Taori S, Zhao Y, Snyder NW, Placantonakis DG and Rich JN. Lactate reprograms glioblastoma immunity through CBX3-regulated histone lactylation. J Clin Invest 2024; 134: e176851.
[19] Wahab MA, Del Gaudio N, Gargiulo B, Quagliariello V, Maurea N, Nebbioso A, Altucci L and Conte M. Exploring the role of CBX3 as a potential therapeutic target in lung cancer. Cancers (Basel) 2024; 16: 3026.
[20] Ma J, Ren D, Wang Z, Li W, Li L, Liu T, Ye Q, Lei Y, Jian Y, Ma B, Fan Y, Liu J, Gao Y, Jin X, Huang H and Li L. CK2-dependent degradation of CBX3 dictates replication fork stalling and PARP inhibitor sensitivity. Sci Adv 2024; 10: eadk8908.
[21] Xiang Y, Mata-Garrido J, Fu Y, Desterke C, Batsché E, Hamaï A, Sedlik C, Sereme Y, Skurnik D, Jalil A, Onifarasoaniaina R, Frapy E, Beche JC, Alao R, Piaggio E, Arbibe L and Chang Y. CBX3 antagonizes IFNγ/STAT1/PD-L1 axis to modulate colon inflammation and CRC chemosensitivity. EMBO Mol Med 2024; 16: 1404-1426.
[22] Bai X, Duan T, Shao J, Zhang Y, Xing G, Wang J, Liu X, Wang M, He Y, Wang H, Zhang ZY, Ni M, Zhou JY and Pan J. CBX3 promotes multidrug resistance by suppressing ferroptosis in colorectal carcinoma via the CUL3/NRF2/GPX2 axis. Oncogene 2025; 44: 1678-1693.
[23] Pu Z, Xu M, Yuan X, Xie H and Zhao J. Circular RNA circCUL3 accelerates the warburg effect progression of gastric cancer through regulating the STAT3/HK2 axis. Mol Ther Nucleic Acids 2020; 22: 310-318.
[24] Pu Z, Wang W, Xie H and Wang W. Apolipoprotein C3 (ApoC3) facilitates NLRP3 mediated pyroptosis of macrophages through mitochondrial damage by accelerating of the interaction between SCIMP and SYK pathway in acute lung injury. Int Immunopharmacol 2024; 128: 111537.
[25] Pu Z, Sui B, Wang X, Wang W, Li L and Xie H. The effects and mechanisms of the anti-COVID-19 traditional Chinese medicine, Dehydroandrographolide from Andrographis paniculata (Burm.f.) Wall, on acute lung injury by the inhibition of NLRP3-mediated pyroptosis. Phytomedicine 2023; 114: 154753.
[26] Pu Z, Shen C, Zhang W, Xie H and Wang W. Avenanthramide C from oats protects pyroptosis through dependent ROS-induced mitochondrial damage by PI3K ubiquitination and phosphorylation in pediatric pneumonia. J Agric Food Chem 2022; 70: 2339-2353.
[27] Rammal R, Seethala R, Gorantla V, Skaugen J, Singhi AD and Naous R. Epithelial-predominant synovial sarcoma with a deceptive neuroendocrine phenotype. Cureus 2025; 17: e82988.
[28] Rajaram M, Babu MV, Gocchait D, Malik A, Mohaptra MM and Vijayarengan NC. Primary synovial sarcoma of lung - a report of two cases. J Family Med Prim Care 2025; 14: 1553-1556.
[29] Mishra C, Gulati A, Nischal N, Gautam D, Javed A and Singh JP. "Tadpole tail sign" in high-grade synovial sarcoma of the ulnar nerve: a case report. J Ultrasound 2025; [Epub ahead of print].
[30] Ozono K, Sakanashi K, Iwamoto N, Nakanishi Y, Oda Y and Nakamura M. A case of primary pulmonary synovial sarcoma. Respir Med Case Rep 2025; 56: 102236.
[31] Yue W, Hua D, Yumei F, Mengyi L, Jian Z, Dajiang S, Shu L and Ke L. Case report: a rare case of male breast synovial sarcoma. Front Oncol 2025; 15: 1469910.
[32] Medina-Ceballos E, Giner F, Machado I, Heras-Morán B, Espino M, Navarro S and Llombart-Bosch A. The prognostic impact of the tumor immune microenvironment in Synovial Sarcoma: an immunohistochemical analysis using digital pathology and conventional interpretation. J Pers Med 2025; 15: 169.
[33] Saito T. The SYT-SSX fusion protein and histological epithelial differentiation in synovial sarcoma: relationship with extracellular matrix remodeling. Int J Clin Exp Pathol 2013; 6: 2272-2279.
[34] Qi Y, Wang N, He Y, Zhang J, Zou H, Zhang W, Gu W, Huang Y, Lian X, Hu J, Zhao J, Cui X, Pang

L and Li F. Transforming growth factor-β1 signaling promotes epithelial-mesenchymal transition-like phenomena, cell motility, and cell invasion in synovial sarcoma cells. PLoS One 2017; 12: e0182680.
[35] Saito T, Nagai M and Ladanyi M. SYT-SSX1 and SYT-SSX2 interfere with repression of E-cadherin by snail and slug: a potential mechanism for aberrant mesenchymal to epithelial transition in human synovial sarcoma. Cancer Res 2006; 66: 6919-6927.
[36] Subramaniam MM, Navarro S and Llombart-Bosch A. Immunohistochemical study of correlation between histologic subtype and expression of epithelial-mesenchymal transition-related proteins in synovial sarcomas. Arch Pathol Lab Med 2011; 135: 1001-1009.
[37] Chen J, Lin Y, Zheng S, Chen Q, Tang S and Zhong X. CBX3 promotes clear cell renal carcinoma through PI3K/AKT activation and aberrant immunity. J Transl Med 2023; 21: 600.
[38] Ebrahimi N, Adelian S, Shakerian S, Afshinpour M, Chaleshtori SR, Rostami N, Rezaei-Tazangi F, Beiranvand S, Hamblin MR and Aref AR. Crosstalk between ferroptosis and the epithelial-mesenchymal transition: implications for inflammation and cancer therapy. Cytokine Growth Factor Rev 2022; 64: 33-45.
[39] Pu Z, Li L, Zhang Y, Shui Y, Liu J, Wang X, Jiang X, Zhang L and Yang H. Exploring the therapeutic potential of HAPC in COVID-19-induced acute lung injury. Phytomedicine 2025; 139: 156563.
[40] Gao M, Lai K, Deng Y, Lu Z, Song C, Wang W, Xu C, Li N and Geng Q. Eriocitrin inhibits epithelial-mesenchymal transformation (EMT) in lung adenocarcinoma cells via triggering ferroptosis. Aging (Albany NY) 2023; 15: 10089-10104.
[41] Lee J and Roh JL. Epithelial-mesenchymal plasticity: implications for ferroptosis vulnerability and cancer therapy. Crit Rev Oncol Hematol 2023; 185: 103964.
[42] Guo W, Duan Z, Wu J and Zhou BP. Epithelial-mesenchymal transition promotes metabolic reprogramming to suppress ferroptosis. Semin Cancer Biol 2025; 112: 20-35.
[43] Igarashi K, Nishizawa H, Saiki Y and Matsumoto M. The transcription factor BACH1 at the crossroads of cancer biology: from epithelial-mesenchymal transition to ferroptosis. J Biol Chem 2021; 297: 101032.
[44] Chen P, Li X, Zhang R, Liu S, Xiang Y, Zhang M, Chen X, Pan T, Yan L, Feng J, Duan T, Wang D, Chen B, Jin T, Wang W, Chen L, Huang X, Zhang W, Sun Y, Li G, Kong L, Chen X, Li Y, Yang Z, Zhang Q, Zhuo L, Sui X and Xie T. Combinative treatment of β-elemene and cetuximab is sensitive to KRAS mutant colorectal cancer cells by inducing ferroptosis and inhibiting epithelial-mesenchymal transformation. Theranostics 2020; 10: 5107-5119.
[45] Chen Z, Li H, Li Z, Chen S, Huang X, Zheng Z, Qian X, Zhang L, Long G, Xie J, Wang Q, Pan W and Zhang D. SHH/GLI2-TGF-β1 feedback loop between cancer cells and tumor-associated macrophages maintains epithelial-mesenchymal transition and endoplasmic reticulum homeostasis in cholangiocarcinoma. Pharmacol Res 2023; 187: 106564.
[46] Huang X, Xu X, Bringas P Jr, Hung YP and Chai Y. Smad4-Shh-Nfic signaling cascade-mediated epithelial-mesenchymal interaction is crucial in regulating tooth root development. J Bone Miner Res 2010; 25: 1167-1178.
[47] Panman L, Galli A, Lagarde N, Michos O, Soete G, Zuniga A and Zeller R. Differential regulation of gene expression in the digit forming area of the mouse limb bud by SHH and gremlin 1/FGF-mediated epithelial-mesenchymal signalling. Development 2006; 133: 3419-3428.
[48] Sun X, Song J, Li E, Geng H, Li Y, Yu D and Zhong C. Cigarette smoke supports stemness and epithelial-mesenchymal transition in bladder cancer stem cells through SHH signaling. Int J Clin Exp Pathol 2020; 13: 1333-1348.
[49] Chatterjee R, Ghosh B, Mandal M, Nawn D, Banerjee S, Pal M, Paul RR, Banerjee S and Chatterjee J. Pathophysiological relationship between hypoxia associated oxidative stress, Epithelial-mesenchymal transition, stemness acquisition and alteration of Shh/Gli-1 axis during oral sub-mucous fibrosis and oral squamous cell carcinoma. Eur J Cell Biol 2021; 100: 151146.